



Effect of Helium on Irradiation Creep Behavior of B-Doped F82H Irradiated in HFIR

M. Ando, T. Nozawa, T. Hirose, H. Tanigawa, E. Wakai, R. E. Stoller & J. Myers

To cite this article: M. Ando, T. Nozawa, T. Hirose, H. Tanigawa, E. Wakai, R. E. Stoller & J. Myers (2015) Effect of Helium on Irradiation Creep Behavior of B-Doped F82H Irradiated in HFIR, *Fusion Science and Technology*, 68:3, 648-651, DOI: [10.13182/FST14-963](https://doi.org/10.13182/FST14-963)

To link to this article: <https://doi.org/10.13182/FST14-963>



Published online: 23 Mar 2017.



Submit your article to this journal [↗](#)



Article views: 46



View related articles [↗](#)



View Crossmark data [↗](#)

EFFECT OF HELIUM ON IRRADIATION CREEP BEHAVIOR OF B-DOPED F82H IRRADIATED IN HFIR

M. Ando,^{a,*} T. Nozawa,^a T. Hirose,^a H. Tanigawa,^a E. Wakai,^a R.E. Stoller,^b and J. Myers^b

^aJapan Atomic Energy Agency, Rokkasho-mura, Aomori-ken, Japan 039-3212,

^bOak Ridge National Laboratory, 1 Bethel Valley Rd, Oak Ridge, TN37831, USA
ando.masami@jaea.go.jp

The diameter of pressurized tubes of F82H and B-doped F82H irradiated up to ~6 dpa have been measured by a non-contacting laser profilometer. The irradiation creep strains of F82H irradiated at 573 and 673K were almost linearly dependent on the effective stress level for stresses below 260 MPa and 170 MPa, respectively. The creep strain of ¹⁰BN-F82H was similar to that of F82H IEA at each effective stress level except 294 MPa at 573K irradiation. For 673K irradiation, the creep strain of some ¹⁰BN-F82H tubes was larger than that of F82H tubes. However, the generation of ~300 appm He did not cause a large difference in the irradiation creep behavior at 6 dpa.

I. INTRODUCTION

Reduced activation ferritic/martensitic steels (RAFM) are the most promising candidates for blanket structural materials of fusion reactors.¹⁻³ Recently, 5 ton and 20 ton large heats of F82H BA heat were manufactured under the Broader Approach (BA) activity by Japan Atomic Energy Agency (JAEA). In addition, neutron irradiation experiments have been completed for the F82H IEA heat, the so-called modify-3 heat and other variants up to ~80 dpa in HFIR. Above all, irradiation creep has been recognized as one of the most important properties for engineering data required for the blanket structural design. For irradiation creep experiments, some results on RAFM (JLF-1 and F82H) above 663K have been reported by the Japan/US collaboration program for fusion structural materials.⁴ For fusion reactors, it is anticipated that irradiation creep of RAFM at lower temperatures (<573K) could be also significant. In a previous study, the irradiation creep of JLF-1 and F82H irradiated at 573K has been reported⁵ and it was obvious that the irradiation creep of RAFM was induced at low temperature (~573K) without thermal creep. Furthermore, some transmutation products (mainly helium atoms) will be also produced by high-energy neutrons in the first wall of a fusion reactor. To investigate the effect of helium on material properties for RAFM, some results of isotope tailoring experiments using the reaction of ¹⁰B(n, α)⁷Li or ⁵⁸Ni(n, γ)⁵⁷Ni(n, α)⁵⁶Fe in RAFM doped with ¹⁰B or ⁵⁸Ni

(Refs. 6-9) and experiments using α particle implantation (~1000 appm) at 393~823K using a cyclotron accelerator¹⁰ have been reported. However, there has been little data on the effects of helium on irradiation creep behavior in ¹⁰B-doped F82H.

The objective of this study is to examine the effects of helium on irradiation creep behavior using pressurized tubes made from F82H in which the isotopes of boron were specifically tailored.

II. EXPERIMENTAL

The materials studied were F82H IEA heat (8Cr-2WVTa) and boron-doped F82H steels provided by JAEA. The chemical compositions and heat treatments of these materials are given in Table I. ¹⁰Boron-doped F82H was provided to investigate the effect of helium on mechanical properties. In this experiment, two types of boron-doped F82H were prepared by a co-doping of boron and nitrogen in F82H steel.^{11, 12} One is ¹⁰BN-F82H which produced helium atoms by the reaction ¹⁰B (n, α) ⁷Li during irradiation. The other is ¹¹BN-F82H which did not produce helium. These BN co-doped F82H steels with modified heat treatments show that mechanical properties were improved by a suppression of boron localization.¹³

TABLE I. Chemical Composition and Heat Treatments of F82H and BN-doped F82H (mass%)

	C	Cr	W	V	Ta	Mn
F82H IEA heat	0.090	7.71	1.95	0.16	0.020	0.16
¹⁰ BN-doped F82H	0.099	8.09	2.10	0.30	0.039	0.10
¹¹ BN-doped F82H	0.088	8.08	2.09	0.31	0.043	0.10

	Si	P	S	N	B	Helium*
F82H IEA heat	0.11	0.002	0.0020	0.006	0.0002	~2
¹⁰ BN-doped F82H	0.10	0.006	0.0008	0.020	0.0059	~300
¹¹ BN-doped F82H	0.11	0.006	0.0010	0.020	0.0053	~10

*Estimation (ppm) for 6 dpa¹⁶

	No	Normalizing	Tempering
F82H IEA heat	-	1313K 40min AC	1023K 1h AC
^{10/11} BN-doped F82H	1st	1423K 30min WQ	973K 2h AC
	2nd	1273K 10min WQ	1053K 30min AC

The tube specimens had dimensions of 4.5 mm outside diameter and 25.4 mm length with a 0.2 mm wall thickness as shown in Figure 1. End caps were electron

beam welded to the tube segments, and the specimens were pressurized with high purity helium (99.999% He) to obtain the desired hoop stresses at the irradiation temperatures. The hoop stresses ranged from 0 to 380 MPa at the irradiation temperature.

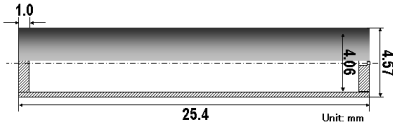


Fig. 1. Geometry of the pressurized tube specimen.

These tubes were fabricated and then the diameter of tubes was measured with a non-contacting laser profilometer system (Beta Lasermike Model 162) capable of a precision of ± 250 nm at Oak Ridge National Laboratory (ORNL) prior to irradiation.

Irradiation was performed in the High Flux Isotope Reactor (HFIR) to atomic displacement levels up to 5.8 dpa at the reactor mid-plane location in the removable beryllium (RB) position. This capsule equipped with a thermal neutron shielded (Eu_2O_3) capsule. As a result, ^{10}B was slowly transmuted to helium in the shielded capsule. Nominal irradiation temperatures were 573 and 673K. These tubes were irradiated in the HFIR from cycle 415 to cycle 424 for an accumulated exposure time of 236 effective full-power days.¹⁴

Each tube was measured three times using a laser profilometer system installed in the ORNL hot cell. The average diameter of the central three-fifths of each tube was used in the analysis of the data. Irradiation creep strain was calculated from tube diameter measured before and after irradiation.

The Vickers hardness test was performed at a load of 9.8 N using an AAV-500 micro-Vickers-hardness tester in Hot cell. The hardness test was 8 ~ 10 points for each SS-J3 tensile specimen at the end tab area.

III. RESULTS AND DISCUSSION

Table II shows the irradiation conditions and results of irradiation creep measurements for pressurized tube specimens irradiated at 573 and 673K. A total of 33 tubes was measured in the hot cell.

For a pressurized tube specimen with biaxial stress state, the effective stress is obtained by:

$$\sigma_{\text{eff}} = \frac{\sqrt{3}}{2} \sigma_{\text{hoop}} \quad (1)$$

where σ_{eff} is the effective uniaxial stress and σ_{hoop} is the hoop stress in the tube wall. Effective creep strain is calculated from the change in the outer diameter of tube after irradiation. Using the measured diameters, the effective creep strain is calculated using the following expression:

$$\epsilon_{\text{eff}} = 1.15 \left[\frac{2}{\sqrt{3}} \right] \frac{\Delta D}{D_0} \quad (2)$$

where ΔD is the change in the tube's outer diameter before and after irradiation, and D_0 is the outer diameter before irradiation.

TABLE II. Irradiation Condition of Pressurized Tubes F82H IEA Heat

Hoop Stress MPa	D_0 inch	ΔD inch	Irradiation Temperature K	Dose dpa
380	0.179751	0.001009	573	3.7
340	0.179489	0.000349	573	4.2
300	0.179922	0.000183	573	3.7
250	0.179174	0.000140	573	4.2
200	0.180122	0.000164	573	4.2
200	0.178894	0.000158	573	4.2
150	0.180132	0.000043	573	3.7
150	0.178956	-0.000071	573	4.2
100	0.179972	0.000010	573	4.2
100	0.178504	0.000136	573	4.2
0	0.179423	0.000053	573	3.7
250	0.179697	0.000619	673	5.7
250	0.178861	0.000438	673	5.7
200	0.180164	0.000283	673	5.7
200	0.180216	0.000217	673	5.7
170	0.178755	0.000270	673	5.7
150	0.179864	0.000097	673	5.7
100	0.178718	0.000131	673	5.7
100	0.179688	-0.000253	673	5.7
0	0.179104	-0.000014	673	5.7

$^{10}\text{BN-F82H}$

340	0.178248	0.000511	573	3.7
250	0.177530	0.000168	573	3.7
200	0.178576	0.000116	573	4.2
150	0.179071	0.000117	573	4.2
0	0.178501	0.000040	573	3.7
250	0.178299	0.000503	673	5.8
200	0.179717	0.000198	673	5.8
150	0.178616	0.000185	673	5.8
0	0.178306	0.000079	673	5.8

$^{11}\text{BN-F82H}$

250	0.179046	0.000359	673	5.8
200	0.178489	0.000189	673	5.8
150	0.179522	0.000137	673	5.8
0	0.179375	-0.000005	673	5.8

The outer diameter strain is converted to the mid-wall strain using a factor of 1.15, and the measured strain is converted to the effective uniaxial strain by the factor $2\sqrt{3}$ (Ref. 15).

Figure 2 shows the relationship between the effective creep strain (ϵ_{eff}) and the effective stress (σ_{eff}) in F82H IEA and BN-F82H irradiated at 573K. F82H IEA and BN-F82H exhibit similar irradiation creep behavior at 573K up to ~4 dpa. The irradiation creep strain in F82H is nearly linearly dependent on the effective stress level for stresses up to ~260 MPa. However, the creep strain becomes nonlinear at higher stress levels.

Figure 3 shows the results of 673K irradiation. In this case, the irradiation creep strain of F82H is linear below ~170 MPa.

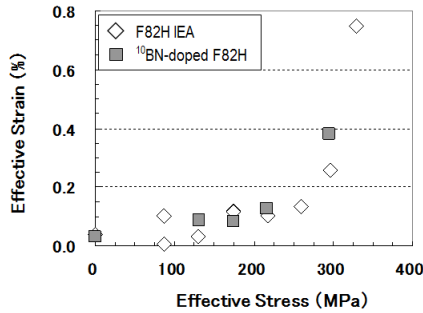


Fig. 2. Relationship between effective strain and effective stress of F82H IEA and BN-doped F82H irradiated at ~573K.

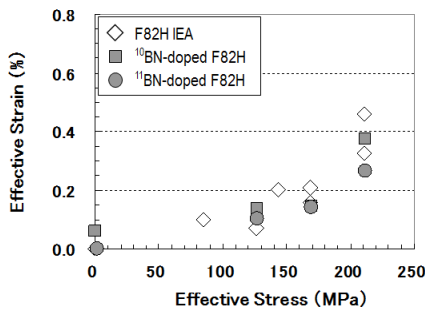


Fig. 3. Relationship between effective strain and effective stress of F82H IEA and BN-doped F82H irradiated at ~673K.

The effect of helium on irradiation creep of F82H was also examined using ¹⁰BN and ¹¹BN-F82H. Helium production during irradiation was estimated to be about 300 appm and its production rate was controlled using a thermal neutron shielded (Eu₂O₃) capsule.¹⁶ The creep strain of ¹⁰BN-F82H was similar to that of F82H IEA at each effective stress level except for ~290 MPa at 573K irradiation. For 673K irradiation, the creep strain of some ¹⁰BN-F82H tubes was larger than that of ¹¹BN-F82H tubes (including the stress free tube). It is suggested that a limited amount of swelling may be induced in ¹⁰BN-F82H because of small helium bubbles arising from the production of helium by the ¹⁰B(n, α)⁷Li reaction. An estimated 0.06% swelling was obtained based on the volume increase of tube. This result is consistent with the swelling expected from a production of small helium bubbles.^{9,17}

Figure 4 shows the result of Vickers hardness for F82H IEA, ¹⁰BN- and ¹¹BN-F82H after neutron irradiation in same capsule. For 573K irradiation, irradiation hardening of ¹⁰BN-F82H is larger than ¹¹BN-F82H because the irradiation dose of ¹⁰BN-F82H was higher than that of ¹¹BN-F82H. However, radiation-induced hardening was also higher in ¹⁰BN-F82H at 673K

irradiation when the dose was the same for both materials. It has been reported that almost no irradiation hardening is observed for F82H after neutron irradiation above 673K. Therefore, it is considered that the hardening of ¹⁰BN-F82H is also primarily caused by very small helium bubbles.

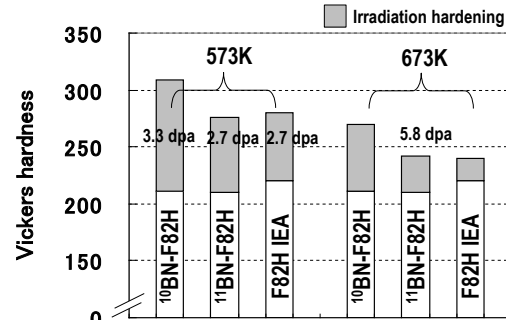


Fig. 4. Irradiation hardening of BN-doped F82H after 573 and 673K irradiation.

These results suggest that high-dose 14 MeV neutron irradiation of F82H at ~673K could have a large impact on the life expectancy of blanket structure because it is possible to create void swelling in F82H around this temperature.^{9,18} Generally, very small bubbles are formed in ¹⁰BN-F82H up to several dpa, and irradiation hardening is caused by these bubbles. However, coarser cavity microstructures (voids + bubbles) after high-dose irradiation do not contribute as much irradiation hardening. Additionally, the irradiation creep can be expressed in the following equation:¹⁹

$$\varepsilon = B\sigma^n\phi t + D\sigma \quad (3)$$

where ϕt is the displacement damage in dpa, S corresponds to the volumetric swelling, B the creep compliance of irradiation creep deformation, and D is the creep-swelling coupling coefficient for irradiation creep deformation. For high-dose irradiation at 673K, the contribution of the factor S in this equation increases. Therefore, it is expected that the creep lifetime may decrease. Furthermore, the microstructure examination of these tube specimens will be also performed to understand the irradiation hardening of ¹⁰BN-F82H by helium at 673K irradiation in future studies.

Figure 5 summarizes the current and reported data of F82H for the relationship between the creep strain rate (%/dpa) and the stress after neutron irradiation. The size of marker indicates the magnitude of irradiation dose. The data for 36 and 60 dpa were obtained by FFTF irradiation.⁴ The current results are shown to be similar to the previously reported data.⁵ If the irradiation creep strain rate (%/dpa) for each irradiation temperature is a

constant value, it is expected that irradiation creep behavior below 573K cannot be neglected after high-dose irradiation. In addition, high-dose irradiation creep data below 573K should be also obtained in the future.

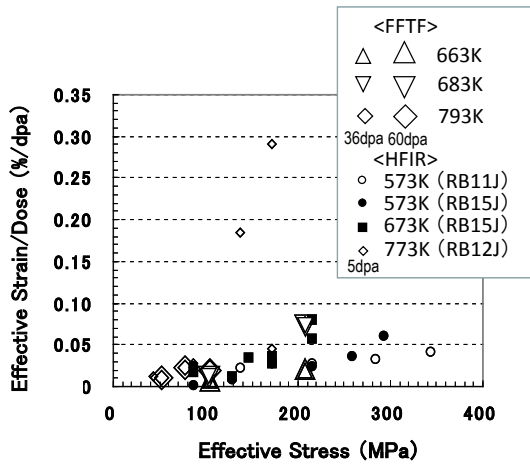


Fig. 5. Summary of irradiation creep data for F82H.

IV. CONCLUSION

Effect of helium on irradiation creep behavior up to 300 appm, ~6 dpa was examined using F82H and BN-doped F82H. The results are summarized below;

- 1) For irradiation at 573K, to 4.2 dpa, the irradiation creep behavior of F82H and ^{10}BN -doped F82H is similar.
- 2) For irradiation at 673K, to 5.8 dpa, the irradiation hardening and creep strain for ^{10}BN -doped F82H was slightly higher. However, they did not cause a large difference in irradiation creep behavior.
- 3) The results of this study will be summarized in a database on the irradiation properties of F82H under the JP-EU Broader Approach (BA) activities. A more accurate assessment of the effects of helium following high-dose irradiation is required; this may be provided by a high-energy neutron source.

ACKNOWLEDGMENTS

This research was sponsored by the Office of Fusion Energy Sciences, U.S. Department of Energy and Japan Atomic Energy Agency, under contract DE-AC05-00OR22725 with UT-Battelle, LLC. The authors would like to thank the assistance of Mr. Patrick S. Bishop and hot cell operators of the ORNL Building 3025 hot cell facility to the experimental work.

REFERENCES

1. M. ENOEDA, et al., *Fusion Eng. Des.*, **89**, 1131-1136 (2014); <http://dx.doi.org/10.1016/j.fusengdes.2014.01.035>.
2. H. TANIGAWA, et al., *J. Nucl. Mater.*, **417**, 9-15 (2011); <http://dx.doi.org/10.1016/j.jnucmat.2011.05.023>.
3. A. KIMURA, et al., *J. Nucl. Mater.*, **367-370**, 60-67 (2007); <http://dx.doi.org/10.1016/j.jnucmat.2007.03.013>.
4. A. KOHYAMA, et al., *J. Nucl. Mater.*, **212-215**, 751-754 (1994); [http://dx.doi.org/10.1016/0022-3115\(94\)90157-0](http://dx.doi.org/10.1016/0022-3115(94)90157-0).
5. M. ANDO, et al., *J. Nucl. Mater.*, **367-370**, 122-126 (2007); <http://dx.doi.org/10.1016/j.jnucmat.2007.03.157>.
6. K. SHIBA, et al., *J. Nucl. Mater.*, **283-287**, 474-477 (2000); [http://dx.doi.org/10.1016/S0022-3115\(00\)00369-X](http://dx.doi.org/10.1016/S0022-3115(00)00369-X).
7. A. KIMURA, et al., *J. Nucl. Mater.*, **307-311**, 521-526 (2002); [http://dx.doi.org/10.1016/S0022-3115\(02\)01211-4](http://dx.doi.org/10.1016/S0022-3115(02)01211-4).
8. N. HASHIMOTO, et al., *J. Nucl. Mater.*, **307-311**, 222-228 (2002); [http://dx.doi.org/10.1016/S0022-3115\(02\)01183-2](http://dx.doi.org/10.1016/S0022-3115(02)01183-2).
9. E. WAKAI, et al., *J. Nucl. Mater.*, **283-287**, 799-805 (2000); [http://dx.doi.org/10.1016/S0022-3115\(00\)00268-3](http://dx.doi.org/10.1016/S0022-3115(00)00268-3).
10. N. YAMAMOTO, et al., *J. Nucl. Mater.*, **307-311**, 217-221 (2002); [http://dx.doi.org/10.1016/S0022-3115\(02\)01182-0](http://dx.doi.org/10.1016/S0022-3115(02)01182-0).
11. E. WAKAI, et al., *J. Nucl. Mater.*, **398**, 64-67 (2010); <http://dx.doi.org/10.1016/j.jnucmat.2009.10.011>.
12. N. OKUBO, *J. Nucl. Mater.*, **367-370**, 107-111 (2007); <http://dx.doi.org/10.1016/j.jnucmat.2007.03.159>.
13. E. WAKAI, et al., *J. Plasma Fusion Res. SERIES*, Vol.11, 104-112 (2015).
14. J. MCDUFFEE, and D. HEATHERLY, *Semiannual Progress Report*, DOE/ER-0313/49, 110-114 (2010).
15. E.R.GILBERT and L.D.BLACKBURN, *J. Eng. Mater. Technol.*, 168 (1977); <http://dx.doi.org/10.1115/1.3443428>.
16. N. HASHIMOTO, et al., *J. Nucl. Mater.*, **307-311**, 222 (2002); [http://dx.doi.org/10.1016/S0022-3115\(02\)01183-2](http://dx.doi.org/10.1016/S0022-3115(02)01183-2).
17. E. WAKAI, et al., *J. Nucl. Mater.*, **307-311**, 203-211 (2002); [http://dx.doi.org/10.1016/S0022-3115\(02\)01261-8](http://dx.doi.org/10.1016/S0022-3115(02)01261-8).
18. E. WAKAI, et al., *J. Nucl. Mater.*, **318**, 267-273 (2003); [http://dx.doi.org/10.1016/S0022-3115\(03\)00122-3](http://dx.doi.org/10.1016/S0022-3115(03)00122-3).
19. D. S. GELLES and R. J. PUIGH, *ASTM STP870*, 19 (1986).